Bisphenol-S and Bisphenol-F alter mouse pancreatic β-cell ion channel expression and activity and insulin release through an estrogen receptor ERβ mediated pathway

Laura Marroqui[1,2], Juan Martinez-Pinna[1,3], Manuel Castellano-Muñoz[2], Reinaldo S. dos Santos[1,2], Regla M. Medina-Gali[1,2], Sergi Soriano[1,3], Ivan Quesada[1,2], Jan-Ake Gustafsson[4,5], José A. Encinar[1] and Angel Nadal[1,2,*].

1. Instituto de Investigación, Desarrollo e Innovación en Biotecnología Sanitaria de Elche (IDiBE), Universitas Miguel Hernández, Elche, Spain.
2. Centro de Investigación Biomédica en Red de Diabetes y Enfermedades Metabólicas Asociadas (CIBERDEM), Spain.
3. Departamento de Fisiología, Genética y Microbiología, Universidad de Alicante, Alicante, Spain.
4. Department of Cell Biology and Biochemistry, Center for Nuclear Receptors and Cell Signaling, University of Houston, Houston, TX, USA.
5. Department of Biosciences and Nutrition, Karolinska Institutet, Huddinge, Sweden

KEYWORDS: Bisphenol, Islet of Langerhans, Endocrine Disrupting Chemicals, Estrogen Receptors, Molecular Dynamics Simulation

ABSTRACT

Bisphenol-S (BPS) and Bisphenol-F (BPF) are current Bisphenol-A (BPA) substitutes. Here we used pancreatic β-cells from wild type (WT) and estrogen receptor β (ERβ) knockout (BERKO) mice to investigate the effects of BPS and BPF on insulin secretion, and the expression and activity of ion channels involved in β-cell function. BPS or BPF rapidly increased insulin release and diminished ATP-sensitive K^+ (K_{ATP}) channel activity. Similarly, 48 h treatment with BPS or BPF enhanced insulin release and decreased the expression of several ion channel subunits in β-cells from WT mice, yet no effects were observed in cells from BERKO mice. PaPE-1, a ligand designed to preferentially trigger extranuclear-initiated ER pathways, mimicked the effects of bisphenols, suggesting the involvement of extranuclear-initiated ERβ pathways. Molecular dynamics simulations indicated differences in ERβ ligand-binding domain dimer stabilization and solvation free energy among different bisphenols and PaPE-1. Our data suggest a mode of action involving ERβ whose activation alters three key cellular events in β-cell, namely ion channel expression and activity, and insulin release. These results may help to improve the hazard identification of bisphenols.

INTRODUCTION

The relationship between BPA exposure and hormone related diseases (Gore et al., 2015) has raised consumers concern. Consequently, BPA has been progressively substituted by other bisphenol analogs. Among the nearly 15 bisphenol analogs, BPS and BPF are widely consumed and commercialized (Rochester and Bolden, 2015), being the major bisphenol contaminants in indoor dust along with BPA (Liao et al., 2012b). Similar to BPA, the detection frequencies of BPS and BPF were approximately 80% in urine samples collected from the general United States population and several Asian countries (Liao et al., 2012a; Ye et al., 2015). In the United States population, the detection frequency of BPS in urine has increased between 2000 and 2014 while that of BPA trends to decrease since 2010. BPA had a frequency and geometric mean concentrations of 74−99% and 0.36−2.07 μg/L, followed by BPF 42−88%, 0.15−0.54 μg/L and BPS, 19−74%, < 0.1−0.25 μg/L (Ye et al., 2015). BPA has a tolerable daily intake (TDI) determined by the European Food Safety Authority in 2015 of 4 μg/kg-day and in 2017 it was identified by the European Chemical Agency as a substance of very high concern due to its endocrine disrupting properties (Beausoleil et al., 2018). Of note, TDIs for other bisphenols do not yet exist.

BPA has been considered a risk factor in the etiology of type 2 diabetes (T2D) (Alonso-Magdalena et al., 2006; Ropero et al., 2008; Nadal et al., 2009; Batista et al., 2012). Epidemiological and prospective studies associated BPA exposure with alterations in glucose homeostasis or T2D incidence, independently of obesity or other traditional factors (Lang et al., 2008; Shankar and Teppala, 2011; Beydoun et al., 2014; Ranciere et al., 2019). Recent epidemiological data associated BPS urine levels with T2D development in a case-cohort study (Ranciere et al., 2019)

and a case-control study (Duan et al., 2018). BPF has been recently associated with abdominal obesity in children (Jacobson et al., 2019), but association with T2D is still unclear.

T2D occurs due to a progressive loss of sufficient β-cell insulin secretion frequently on the background of insulin resistance (American Diabetes, 2018). The use of animal and cellular models indicated a link between BPA exposure and diabetes development (Nadal et al., 2009; Alonso-Magdalena et al., 2011; Le Magueresse-Battistoni et al., 2018). Adult male mice exposed to environmentally relevant doses of BPA presented insulin resistance and hyperinsulinemia in fed state (Alonso-Magdalena et al., 2006; Batista et al., 2012). Furthermore, BPA directly affected β-cell function (Quesada et al., 2002; Alonso-Magdalena et al., 2008; Soriano et al., 2012; Martinez-Pinna et al., 2019). Pancreatic β-cells are excitable cells and, therefore, their electrical activity rules stimulus-secretion coupling. A primary event in the mechanism of insulin release is the blockade of the ATP-sensitive K^+ (K_{ATP}) channels, which control β-cell resting membrane potential. This blockade leads to a typical electrical activity pattern consisting of bursts of action potentials produced by the opening of voltage-gated, Ca^{2+}, Na^+ and K^+ channels, as well as a rise in intracellular Ca^{2+}, which culminates in insulin exocytosis (Rorsman and Ashcroft, 2018). Changes in the expression and/or function of these ion channels result in altered insulin secretion and constitute a serious risk factor for T2D (Hiriart et al., 2014; Jacobson and Shyng, 2020).

Even though BPA may act through different modes of action, it is considered a xenoestrogen able to bind to ERβ and ERα (Wetherill et al., 2007). Both ERs exert their actions through nuclear- and extranuclear-initiated pathways. The nuclear-initiated pathway consists of the direct binding of the ligand bound-ERs to estrogen response elements, which are located in the regulatory regions of ER target genes (Smith and O'Malley, 2004; Heldring et al., 2007). Transcriptional regulation also occurs through tethering of ERs to DNA-bound transcription factors AP-1 and Sp-1 (Ascenzi et

al., 2006). Conversely, extranuclear-initiated pathways involve the activation of intracellular signaling cascades that will lead to different effects, including transcriptional regulation (Levin and Hammes, 2016). Although the role of extranuclear-initiated events triggered by environmental estrogens remains poorly understood, rodent models and human studies indicate that this pathway may be important to initiate effects at low doses (Alonso-Magdalena et al., 2008; Vinas and Watson, 2013; Acconcia et al., 2015; Nadal et al., 2018).

In β-cells, nanomolar (1-10nM) concentrations of BPA rapidly (within 10 minutes) block K_{ATP} channels and enhance glucose-stimulated insulin secretion (GSIS) in an ERβ-dependent mechanism (Soriano et al., 2009; Soriano et al., 2012). Longer exposures to BPA (48 hours) regulate gene expression of Ca^{2+}, Na^{+} and K^{+} channels, altering electrical activity, Ca^{2+} signaling, and insulin release (Villar-Pazos et al., 2017; Martinez-Pinna et al., 2019). In addition, BPA exposure for 48 h also increases β-cell division in vivo as well as in primary cells. These effects are mimicked by ERβ agonists and abolished in cells from ERβ knockout mice (BERKO), which do not express ERβ in β-cells, suggesting that ERβ activation is necessary for BPA effects in pancreatic β-cells (Boronat-Belda et al., 2020).

Here we studied BPS and BPF effects on insulin release, and ion channel expression and activity in β-cells from wild type (WT) and BERKO mice. Because evidence suggested an important role of ERβ via an extranuclear-initiated pathway, we compared effects elicited by bisphenols with those induced by Pathway Preferential Estrogen-1 (PaPE-1), a compound that binds to ERs and acts preferentially through extranuclear-initiated pathways (Madak-Erdogan et al., 2016). Additionally, we performed molecular docking and dynamic simulations of bisphenols, PaPE-1 and E2 bound to the ERβ ligand-binding domain (LDB) to evaluate the consistencies and variances among these ligands at the molecular level.

MATERIALS AND METHODS

Chemical substances

Bisphenol-A was obtained from MP Biomedicals (Cat No 155118; Santa Ana, CA, USA). BPS (Cat No 103039), BPF (Cat No 51453), PaPE-1 (Cat No SML1876), and collagenase (Cat No C9263) were obtained from Sigma-Aldrich (Barcelona, Spain). Bisphenols and PaPE-1 were weekly prepared by dissolution in DMSO (used as vehicle).

Animals, islet culture and dispersed islet cells All adult male mice were kept under standard housing conditions (12 h light/dark cycle, food *ad libitum*). BERKO mice were generated as described previously (Krege et al., 1998) and supplied by Jan-Ake Gustafsson's laboratory. Both WT littermates and BERKO mice were acquired from the same supplier and colony. Mice were sacrificed and islets were isolated as previously described (Nadal and Soria, 1997). For patch-clamp experiments, islets were dispersed into single cells and plated on glass coverslips as described before (Valdeolmillos et al., 1992). Cells were kept at 37 °C in a humidified atmosphere of 95% O_2 and 5% CO_2 and used within 48 h of culture. Experimental procedures were performed according to the Spanish Royal Decree 1201/2005 and the European Community Council directive 2010/63/EU. The ethical committee of Miguel Hernandez University reviewed and approved the methods used herein (approvals ID: UMH-IB-AN-01–14 and UMH-IB-AN-02-14).

Glucose-stimulated insulin secretion (GSIS) GSIS was performed in islets as previously described (Santin et al., 2016) with slight changes. Briefly, islets were preincubated for 1 h in glucose-free Krebs-Ringer solution. Afterward, islets were sequentially stimulated with 2.8, 8.3, and 16.7 mM glucose for 1 h either in the presence or absence of treatments (as described in Figure 1). Insulin release and insulin content were measured in islet-free supernatants and acid ethanol-

127 extracted islets lysates, respectively, using a mouse insulin ELISA kit (Mercodia, Uppsala,
128 Sweden).

129 **Patch-clamp recordings** K_{ATP} channel activity was recorded using standard patch-clamp
130 recording procedures from isolated β-cells as described previously (Valdeolmillos et al., 1992;
131 Vettorazzi et al., 2016). Around 80-90% of the single cells were identified as β-cells. Currents
132 were recorded using an Axopatch 200B patch-clamp amplifier (Axon Instruments Co. CA, USA).
133 Patch pipettes were pulled from borosilicate capillaries (Sutter Instruments Co. CA, USA) using a
134 flaming/brown micropipette puller P-97 (Sutter Instruments Co. CA, USA) with resistance
135 between 3–5 MΩ when filled with the pipette solutions as specified below. Bath solution contained
136 (in mM): 5 KCl, 135 NaCl, 2.5 CaCl2, 10 Hepes and 1.1 $MgCl_2$ (pH 7.4) and supplemented with
137 glucose as indicated. The pipette solution contained (in mM): 140 KCl, 1 $MgCl_2$, 10 Hepes and 1
138 EGTA (pH 7.2). The pipette potential was held at 0 mV throughout recording. K_{ATP} channel
139 activity was quantified by digitizing 60 s sections of the current record, filtered at 1 kHz, sampled
140 at 10 kHz by a Digidata 1322A (Axon Instruments Co. CA, USA), and calculating the mean open
141 probability of the channel (NP_o) during the sweep. Channel activity was defined as the product of
142 N, the number of functional channels, and P_o, the open-state probability. Po was determined by
143 dividing the total time channels spent in the open state by the total sample time.
144 For the patch-clamp recordings of voltage-gated Ca^{2+} currents, the whole-cell patch-clamp
145 configuration was used as described previously (Villar-Pazos et al., 2017). Pancreatic β-cells were
146 identified by size (>5 pF) and the corresponding steady-state inactivation properties of the
147 tetrodotoxin (TTX)-sensitive Na^+ current. Data were obtained using an Axopatch 200B patch-
148 clamp amplifier (Axon Instruments Co. CA, USA). Patch pipettes were pulled from borosilicate
149 capillaries (Sutter Instruments Co. CA, USA) using a flaming/brown micropipette puller P-97

(Sutter Instruments Co. CA, USA) and heat polished at the tip using an MF-830 microforge (Narishige, Japan). The bath solution contained 118 mM NaCl, 20 mM TEA-Cl, 5.6 mM KCl, 2.6 mM CaCl2, 1.2 mM MgCl2, 5 mM HEPES and 5 mM glucose (pH 7.4 with NaOH). The pipette solution consisted of 130 mM CsCl, 1 mM CaCl2, 1 mM MgCl2, 10 mM EGTA, 3 mM MgATP and 10 mM HEPES (pH 7.2 with CsOH). After filling the pipette with the pipette solution, the pipette resistance was 3–5 MΩ. A tight seal (>1 GΩ) was established between the β-cell membrane and the tip of the pipette by gentle suction. The series resistance of the pipette usually increased to 6–15 MΩ after moving to whole-cell. Series resistance compensation was used (up to 70%) for keeping the voltage error below 5 mV during current flow. Voltage-gated Ca^{2+} currents were compensated for capacitive transients and linear leak using a -P/4 protocol. Data were filtered (2 kHz) and digitized (10 kHz) using a Digidata 1322 A (Axon Instruments Co. CA, USA) and stored in a computer for subsequent analysis using commercial software (pClamp9, Axon Instruments Co. CA, USA). Experiments were carried out at 32–34 °C.

Quantitative real-time PCR Total RNA was isolated using the RNeasy Micro Kit (Qiagen) and reverse-transcribed using the High Capacity cDNA Reverse Transcription Kit (Applied Biosystems). Quantitative PCR was performed using the CFX96 Real Time System (Bio-Rad, Hercules, CA) as described previously (Villar-Pazos et al., 2017). *Hprt* was used as housekeeping gene. The CFX Manager Version 1.6 (Bio-Rad) was used to analyse the values, which were expressed as relative expression ($2^{-\Delta\Delta Ct}$). The primers used herein have been previously described (Martinez-Pinna et al., 2019).

Molecular docking and dynamics simulations Crystallographic structure of the rat ERβ LBD in complex with pure antiestrogen ICI 164,384 [rERβ-ΔH12-LBD; UniProt code: Q62986, Protein Data Bank (PDB) code: 1HJ1] was used for molecular docking and long-time dynamic (1 μs)

simulation purposes. The missing residues in the 1HJ1 structure (364-377) and the missing side chains (M242, K255, K269, E326, S363, S378, R379, K380 and K435) were reconstructed after generating a homology model at the Swiss-Model server (Biasini et al., 2014; Galiano et al., 2016). Structure of estradiol-bound rat ERβ LBD in complex with LXXLL motif from NCOA5 (rERβ-LBD; UniProt code: Q62986, PDB code: 2J7X) was used for molecular docking and short-time dynamic (100 ns) simulation purposes. The missing residues in the 2J7X structure (239-241 and 369-374) and the missing side chains (V237, M242, K255, E376, R374, K398, and K426) were reconstructed after generating a homology model at Swiss-Model server (Biasini et al., 2014; Galiano et al., 2016) using the 2J7X structure as a template. Molecular docking and dynamics simulations were carried out using YASARA structure v19.9.17 software as previously described (Encinar et al., 2015; Galiano et al., 2016; Ruiz-Torres et al., 2018). The ligand-protein interactions have been detected with the Protein–Ligand Interaction Profiler (FLIP) algorithm (Salentin et al., 2015). Foldx 5.0-calculated (Delgado et al., 2019) was used for frequency distributions of intermolecular protein interaction energy for the subunits of the rERβ-ΔH12-LBD dimer in the presence of different ligands in each LBD cavity (Figure S5).

Data analysis The GraphPad Prism 7.0 software (GraphPad Software, La Jolla, CA, USA) was used for statistical analyses. Data are presented as the mean ± SEM. Statistical analyses were performed using Student's t-test or one-way ANOVA. p values ≤ 0.05 were considered statistically significant.

RESULTS

BPS and BPF affect insulin release

Previous data indicate that treatment with 1 nM BPA rapidly enhances insulin secretion in islets from mice and humans (Alonso-Magdalena et al., 2006; Soriano et al., 2012). To investigate whether BPS and BPF would have similar effects, we treated islets during 1 h with two concentrations of BPS and BPF (1 nM and 1 µM), and we measured insulin release in response to different glucose concentrations (2.8, 8.3 and 16.7 mM). Exposure to 1 nM and 1 µM BPS enhanced GSIS at stimulatory glucose concentration, mainly at 16.7 mM (**Figure 1A**). Regarding BPF, we observed a slight increase at 1 nM that was significant only in the presence of 16.7 mM glucose. BPF 1 µM, however, increased GSIS at both 8.3 and 16.7 mM glucose (**Figure 1B**). We used BPA as a positive control and 1 nM BPA increased GSIS, as expected (**Figure S1A**). Of note, insulin content remained unchanged upon treatment with BPS, BPF, and BPA (**Figure S1C-E**). Longer BPA treatment (48 h) induced insulin hypersecretion in response to stimulatory glucose concentrations (Alonso-Magdalena et al., 2008; Villar-Pazos et al., 2017). We then investigated whether treatment with BPS or BPF during 48 h would also change GSIS. BPS at 1 nM and 1 µM enhanced insulin secretion in response to 8.3 mM glucose. However, when glucose concentration was increased to 16.7 mM, BPS was effective at 1 nM but ineffective at 1 µM (**Figure 1C**). When the same experiment in Figure 1C was performed with BPF, we only observed a potentiation of insulin release at 1 µM at stimulatory glucose concentrations (**Figure 1D**), which indicated a more potent action of BPS compared to BPF. Treatment with BPA, BPS or BPF did not modify insulin content (**Figure S1F-H**).

BPS and BPF diminish K_{ATP} channel activity via ERβ

We have previously demonstrated that acute BPA treatment potentiated GSIS after decreasing K_{ATP} channel activity (Soriano et al., 2012). Moreover, BPA effects, which were not observed in cells from BERKO mice, were reproduced by the endogenous ligand, 17β-estradiol (E2), as well as the ERβ agonist diarylpropionitrile (DPN) (Soriano et al., 2009; Soriano et al., 2012). Acute treatment with BPS induced a rapid increase in heart rate in response to catecholamines (Gao et al., 2015). BPS also rapidly depressed left ventricular contraction and myocyte contractility (Ferguson et al., 2019). In both cases, the ERβ antagonist PHTPP abolished BPS actions, suggesting the involvement of ERβ (Gao et al., 2015; Ferguson et al., 2019).

To assess whether acute exposure to BPS or BPF would modulate K_{ATP} channel activity, we performed patch-clamp recordings in the cell-attached mode in dispersed β-cells from WT and BERKO mice (**Figure 2**). Treatment with 1 nM BPS during 10 minutes was enough to decrease K_{ATP} channel activity by 35% (**Figure 2A**,**B**), whereas no effects were observed in cells from BERKO mice (**Figure 2A**,**C**). A similar experiment was performed using 1 nM and 10 nM BPF. While 1 nM BPF did not modify K_{ATP} channel activity in β-cells from WT and BERKO (data not shown), 10 nM BPF decreased K_{ATP} channel activity in cells from WT (**Figure 2D**) but not in cells from BERKO mice (**Figure 2E**). These findings indicate that the rapid GSIS enhancement observed in **Figure 1A** may be a consequence of bisphenol-induced K_{ATP} channels closure.

The fact that this is a rapid action, occurring minutes upon treatment, indicates that low concentrations of bisphenols trigger a non-genomic action via an extranuclear-initiated pathway, likely by binding to ERβ. To test this hypothesis we used PaPE-1, a new ERα and ERβ ligand that acts preferentially through extranuclear-initiated pathways (Madak-Erdogan et al., 2016). Treatment with 1 μM PaPE-1 decreased K_{ATP} channel activity in cells from WT mice (**Figure 2F**) but had no effect in cells from BERKO mice (**Figure 2G**). Of note, 1 nM PaPE-1 did not change

239 K_{ATP} channel activity (data not shown). These results emphasize that PaPE-1 triggers a rapid
240 extranuclear-initiated pathway via ERβ in β-cells.

241 **Bisphenols downregulate ion channel subunits gene expression**

242 Stimulus-secretion coupling in β-cells depends on the electrical activity generated by ion channels.
243 BPA treatment for 48 h decreased the mRNA expression of genes encoding Ca^{2+} (*Cacna1e*), K^+ (
244 *Kcnma1* and *Kcnip1*) and Na^+ (*Scn9a*) channel subunits, which might explain, at least in part, the
245 BPA-induced alteration in GSIS (Villar-Pazos et al., 2017; Martinez-Pinna et al., 2019). In Figure
246 3 A,E,I) we used BPA as a control to probe that in this preparation it decreased *Cacn1e*, *Kcnma1*,
247 *Kcnip* and *Scn9* as already described (Villar-Pazos et al., 2017; Martinez-Pinna et al., 2019). We
248 found that BPS modulated *Cacna1e* mRNA expression in a non-monotonic dose response
249 (NMDR)-dependent manner: exposure to 1 nM BPS reduced *Cacna1e* mRNA expression by 50%,
250 while exposure to 100 nM and 1 µM did not significantly change *Cacna1e* expression (**Figure**
251 **3B**). This BPS-induced decrease in *Cacna1e* expression at 1 nM was associated to a reduction in
252 Ca^{2+} currents in cells from WT (**Figure S2A,C,I**), but not in cells from BERKO (**Figure S2B,D,I**)
253 mice. Of note, 100 nM and 1 µM BPS did not modify Ca^{2+} currents in cells from WT or BERKO
254 mice (**Figure S2**). It is very likely that the decrease in Ca^{2+} currents induced by 1 nM BPS is a
255 consequence of *Cacna1e* gene downregulation because both follow the same dose pattern.
256 Regarding BPF, *Cacna1e* mRNA expression was not changed by treatment with 1 nM BPF for 48
257 h, but it was decreased upon exposure to 100 nM and 1 µM BPF (**Figure 3C**). Measurement of
258 Ca^{2+} currents showed that only exposure to 1 µM BPF significantly decreased Ca^{2+} currents in
259 cells from WT mice (**Figure S3A,G,I**), while no effects were observed in cells from BERKO mice
260 (**Figure S3B,H,J**). Once again, we used PaPE-1 to study the possible involvement of an
261 extranuclear-initiated pathway in the regulation of *Cacna1e* expression. Treatment with 1 µM

PaPE-1 decreased *Cacna1e* expression (**Figure 3D**), which indicates that this gene can be regulated by a signaling pathway initiated outside the nucleus.

Like what we observed for *Cacna1e* expression, *Kcnma1* (**Figure 3E-H**), *Kcnip1* (**Figure 3I-L**), and *Scn9a* (**Figure 3M-P**) mRNA expression was downregulated by BPA, BPS, BPF and PaPE-1. BPS decreased *Kcnma1*, *Kcnip1*, and *Scn9a* at 1 nM in an NMDR manner, while BPF and PaPE-1 were effective at 1 μM (**Figure 3**).

As a negative control, we used 4,4'-(9-fluorenylidene)diphenol, BPFL (also named BHPF), which binds to the androgen receptor and acts as an antiestrogen (Zhang et al., 2017; Keminer et al., 2019). As expected, BPFL treatment at different concentrations did not change ion channel gene expression or Ca^{2+} currents (**Figure S4**).

Overall, these results demonstrate that BPS decreased the transcription of ion channel subunits at concentrations as low as 1 nM, while BPF needed higher concentrations (100 nM and 1 μM) to decrease the expression of the same genes. This effect was mimicked by PaPE-1, suggesting that bisphenols may regulate gene expression via extranuclear ERs.

We previously used β-cells from BERKO mice as well as the ERβ ligand DPN to study the role of ERβ on the regulation of ion channel subunit gene expression induced by BPA (Villar-Pazos et al., 2017; Martinez-Pinna et al., 2019). To evaluate whether ERβ would also play a role in BPS- and BPF-induced regulation of ion channel expression, we incubated islets from WT and BERKO mice with 1 nM BPS or 1 μM BPF for 48 h. Similarly, to the results depicted in **Figure 3**, both 1 nM BPS and 1 μM BPF decreased *Cacna1e*, *Kcnma1* and *Scn9a* mRNA expression in islets from WT mice (**Figure 4 A-C**). This decrease, however, was abolished in islets from BERKO mice (**Figure 4 D-F**). Notably, 1 μM BPF increased *Cacna1e* expression in BERKO mice, suggesting a role for receptors other than ERβ in the regulation of this gene.

Molecular dynamics simulations of bisphenols bound to the rat ERβ LBD cavity.

To investigate potential modifications in bisphenols and PaPE-1 binding to ERβ ligand binding domin (LBD) that might help to, at least partially, explain the different biological activity of bisphenols observed herein, we performed computational analyses of molecular docking and dynamics simulations.

Despite the numerous studies using human ERα structures on molecular dynamics simulations (Celik et al., 2007; Fratev, 2015; Chen et al., 2016; Jereva et al., 2017; Li et al., 2018; Shtaiwi et al., 2018), the ERβ isoform has not yet been analyzed. Furthermore, ERα LBD and ERβ LBD have not been crystallized in mice, even though the resolved rat structure is well known. Because rat and mouse ERβ LBD sequences differ by only 3 amino acids, including two conservative mutations (**Figure S5A,B**), we chose to use rat structures in our analyses. A recent study using E2, BPA, BPS and BPAF indicated that the root mean square deviation (RMSD) values calculated from the heavy atoms of the ligands might be an important parameter to analyze ligand dynamics particularly implicated in nuclear-initiated events (Li et al., 2018). Therefore, to evaluate if our results fixed with a classic nuclear initiated event, we first studied molecular dynamics simulation of the transactivation helix (H12) closed rERβ-LBD. The natural ligand E2 showed no deviations from the starting configuration for over 100 ns (**Figure S6**), whereas deviations reached 2 Å in the presence of the Src coactivator peptide (**Figure S6**). Meanwhile, rearrangements in conformations are evident from the ligand heavy atom RMSDs in all three bisphenols. In addition, we observed that BPA and BPF showed rapid variations due to faster ring-flipping dynamics (**Figure S6A-C**), similarly to what has been previously shown (Li et al., 2018). The repositioning of H12 in the "mouse trap" conformation decisively influences the MM/PBSA solvation binding energy (Celik et al., 2007). We observed that the solvation binding energy for E2 and BPA was higher than that

for BPS and BPF (**Figure S7**). Interestingly, BPS presented the lowest solvation binding energy value; thus, BPS should bind with lower affinity than BPF and BPA to this configuration, as experimentally demonstrated for the nuclear-initiated pathway (Molina-Molina et al., 2013). These results contrast with the order in biological activity described herein, where we find regulation of ion channel gene expression with at least 100-fold lower concentrations of BPS than BPF. Therefore, a different mechanism to the classic nuclear-initiated event involved in the regulation of ion channel activity and gene expression in β-cells might be implicated in BPS and BPF effects. We then sought to study differences and similarities among E2, BPA, BPS, BPF, and PaPE-1, using what we named rERβ-ΔH12-LBD (PDB code: 1HJ1; (Pike et al., 2001)) dimer complex, and performing long-time (1 μs) molecular dynamics simulations **(Figure 5A)**. In the rERβ-ΔH12-LBD complex, binding of the antiestrogen ICI 164,384 abrogates the association between H12 and the remainder of the LBD, and inhibits both of ER's transactivation functions (AF1 and AF2) (Pike et al., 2001). BPA does not stabilize ERα in a conformation that initiates nuclear events because BPA does not stabilize H12 (Delfosse et al., 2012). Then, simulating binding to rERβ-ΔH12-LBD dimer complex should be convenient to study extranuclear-initiated events.

Dimerization has been demonstrated to be necessary for ERs-mediated extranuclear responses (Razandi et al., 2004; Levin and Hammes, 2016). In our model, BPA, BPS and E2 showed similar frequency distributions of intermolecular protein interaction for both subunits of the dimers, whereas BPF and PaPE-1 presented lower frequency distribution (**Figure 5B**). This suggests a higher stability of the dimers with BPA, BPS and E2. Trajectories of the ligands docked in the LBD cavities (RMSD, Å) are similar except for PaPE-1 (**Figure 5C**), which left the open cavity of the LBD in both subunits after 700 ns (**Figure 5C**) and 840 ns (**Figure 5D**). For E2 and bisphenols, rearrangements rarely exceed 6 Å, indicating that the movement of the ligands into the

cavity is limited, even when H12 is not closing the cavity. Notably, PaPE-1 MM/PBSA solvation binding free energy values, 60 kcal/mol (**Figure 5E**) and 65 kcal/mol (**Figure 5F**), indicate that this compound binds to the protein strongly than bisphenols and E2. On the other hand, bisphenols and E2 remain inside the cavity throughout the entire 1 μs molecular dynamics simulation. We found very similar MM/PBSA solvation binding free energy values for E2 and BPA (around 55 kcal/mol), whereas BPS and BPF presented lower values (45 and 38 kcal/mol, respectively) (**Figure 5E,F**). The solvation binding energies correlated with the number of hydrogen bonds between the protein and the solvent (**Figure 5G)**. BPF presented the lowest solvation binding energy (**Figure 5E,F**) as well as the lowest number of hydrogen bonds (around 680 H-bonds, **Figure 5G**). These results indicate that BPF and PaPE-1 stabilize the ERβ-LBD dimer to a lesser extent than E2, BPA and BPS, which correlates with the lower biological activity observed for BPF and PaPE-1 in the present study. Therefore, we hypothesize that binding of bisphenols to the ERs induces a conformational change that favors an extranuclear-initiated action after dimerization of ERβ.

DISCUSSION

In the present study we found that acute and long-term exposure of primary male mouse β-cells to BPS and BPF led to alterations in β-cell physiology across different levels of biological complexity, including K_{ATP} channel activity, Na^+, K^+ and Ca^{2+} channel subunits expression, and glucose-stimulated insulin release.

Although BPS and BPF have been used as alternatives to BPA, these chemicals may share some of the effects induced by BPA due to their similar structure (Malaise et al., 2020; Mustieles et al.,

2020) or induce different effects to BPA (Kolla et al., 2018). We observed that, similarly to BPA, BPS and BPF enhanced GSIS either after acute treatment (1 h) or upon exposure for 48 h.

The acute effect occurs at the two doses tested, 1 nM and 1 μM, and showed glucose dependence. Bisphenols had no effects at a non-stimulatory glucose concentration (3 mM), had a moderate effect at intermediate glucose concentration (8.3 mM), and had a stronger effect at high glucose (16.7 mM). This potentiation was likely a consequence of the blockade of K_{ATP} channels demonstrated using patch-clamp experiments in the cell-attached mode. In β-cells, K_{ATP} channels control the resting membrane potential. As a result of glucose metabolism, the rise in the ratio ATP/ADP blocks K_{ATP} channels and depolarizes the plasma membrane, thus initiating the electrical activity in burst of action potentials that culminates in insulin release. Here we show that BPS- and BPF-induced blockade of K_{ATP} channels seems to potentiate the effect of glucose on insulin secretion, which leads to insulin hypersecretion.

The rapid BPA-induced potentiation of GSIS has been demonstrated in primary mouse and human β-cells (Soriano et al., 2012). In addition, oral BPA administration rapidly altered insulin and C-peptide levels in blood of adult individuals (Stahlhut et al., 2018; Hagobian et al., 2019). As in the present work BPS and BPF act akin to BPA in β-cells, an analogous effect on human cells might be expected. It is difficult to predict how this rapid action relates to the development of metabolic disorders. Pancreatic β-cells acutely exposed to bisphenols secrete more insulin than untreated cells, which may result in supraphysiological insulin signaling in some target tissues, such as adipose tissue.

Although human evidence are still scarce, BPS has been linked to T2D (Ranciere et al., 2019), while BPS and BPF urine levels have been associated with the prevalence of obesity in children (Jacobson et al., 2019; Liu et al., 2019). In any case, bisphenol-induced insulin hypersecretion may

be one of the altered processes contributing to insulin resistance, which represents a risk factor for both T2D and obesity (Alonso-Magdalena et al., 2006; Corkey, 2012; Erion and Corkey, 2017). BPS and BPF trigger their rapid actions at concentrations as low as 1 nM. In the presence of 16.7 mM glucose, both 1 nM BPS and BPF increased insulin secretion. However, in the presence of 8.3 mM glucose 1 nM BPS potentiated GSIS, while 1 nM BPF did not affect insulin release. These findings indicate that BPF has a slightly lower potency than BPS, which is manifested by the lack of BPF effect at 1 nM on K_{ATP} channel activity. The difference in potency seems to be small since 10 nM BPF blocked K_{ATP} channel activity to a similar extent as 1 nM BPS. Remarkably, bisphenol-induced blockade of K_{ATP} channels was abolished in cells from BERKO mice. BERKO mice β-cells do not express ERβ (Boronat-Belda et al., 2020). Our previous studies demonstrated that 1 nM of E2, DPN, or BPA similarly affected K_{ATP} channel activity (Soriano et al., 2009; Soriano et al., 2012). These data suggest that ERβ activation blocks K_{ATP} channels and that binding to ERβ may mediate the acute action of bisphenols. It is unlikely that this fast response, reached in only 10 minutes, depends on transcriptional regulation; on the contrary, it most likely relies on extranuclear-initiated pathways involving ERβ. Our findings with PaPE-1 and molecular dynamics as well as the existence of a pool of ERβ outside the nucleus of mouse β-cells (Alonso-Magdalena et al., 2008) support this statement. Designed to selectively trigger extranuclear-initiated pathways, PaPE-1 was obtained after chemical rearrangement of key elements of the original steroid structure of E2 so that its ER binding affinity was considerably reduced (Madak-Erdogan et al., 2016). These modifications were performed by substituting the B-ring of the steroid and methylating the positions 2 and 6 of the A-ring, which prevents the formation of key hydrogen bonds within the ligand binding domain (Madak-Erdogan et al., 2016). Similar methylations are observed in tetramethyl BPF (TMBPF), which had no estrogenic effect as assayed by E-SCREEN and it has

399 been proposed as a safer substitute of BPA (Soto et al., 2017). Here, PaPE-1 blocked K_{ATP} channels
400 in islet cells from WT but not from BERKO mice, which indicates that PaPE-1 and bisphenols
401 activate a similar pathway.
402 How can bisphenols trigger a rapid effect at low nanomolar concentrations when their affinity for
403 ERβ is within the micromolar range? It is important to bear in mind that the maximum response
404 to a ligand does not depend exclusively on the receptor affinity. The efficacy of the conformational
405 change needed to initiate the signaling cascade as well as the coupling to other signaling proteins
406 also play key roles in the ligand-receptor response (Colquhoun, 1998). Even though the details of
407 the whole pathway from ERβ activation to K_{ATP} closure is not completely known, it has been
408 shown that 1 nM E2 closes K_{ATP} channels through an extranuclear-initiated pathway that involved
409 ERβ, membrane guanylate cyclase, cGMP formation and protein kinase G activation (Ropero et
410 al., 1999; Soriano et al., 2009). The efficacy of this pathway is extremely high as explained below.
411 In addition to the control of the β-cell resting membrane potential, K_{ATP} channels determine the
412 electrical resistance of the β cell membrane (Ashcroft, 2005). When K_{ATP} channels are open, the
413 electrical resistance is low, whereas the resistance is high when these channels are closed. The
414 membrane potential follows Ohm's law, being the product of the electrical resistance of the
415 membrane by the current running across it. This means that, when extracellular glucose is high,
416 K_{ATP} channels are mostly closed and membrane resistance is high. Hence, a small change in
417 current will elicit membrane depolarization, potentiation of electrical activity, and insulin secretion
418 (Ashcroft, 2005). Our results suggest that bisphenol-induced K_{ATP} channel blockade may lead to
419 enough change in current that will culminate with increased insulin secretion at high glucose. A
420 similar phenomenon is observed with the incretin GLP-1, which acts as an effective secretagogue
421 only when glucose concentrations are stimulatory and a high percentage of K_{ATP} channels are

already closed (Holz et al., 1993). Therefore, low doses of bisphenols will be mainly effective under conditions of decreased K_{ATP} channel activity, as seen in the postprandial state. Accordingly, we show that bisphenols are effective insulin secretagogues only when glucose levels are high.

Besides their acute effects, longer treatment with bisphenols elicited changes in gene expression and GSIS. As already mentioned, insulin release is a consequence of the electrical activity of pancreatic β-cells, which is determined by the expression of ion channels as well as their biophysical characteristics. Both BPS and BPF decreased the expression of *Cacna1e*, *Kcnma1* and *Scn9a,* which encode essential subunits of $Ca_v2.3$, $K_{Ca}1.1$, and $Na_v1.9$ channels. BPS decreased the expression of all channel subunits analyzed at 1 nM, while its effect was lower at 100 nM and 1 µM, which suggests an NMDR relationship. BPF, however, needed higher doses (at least 100 nM) to change channel subunits expression. Therefore, BPS effects on gene expression were 100- and 1000-fold stronger than BPF.

Changes in ion channel expression by 1nM BPA during 48 hours enhanced GSIS (Villar-Pazos et al., 2017; Martinez-Pinna et al., 2019). Here, BPS treatment for 48 h increased GSIS at 1 nM and 1 µM in the presence of 8.3 mM glucose, but only 1 nM BPS was effective in the presence of 16.7 mM glucose. This was surprising and it may indicate the existence of a BPS-triggered mechanism that depends on glucose concentration. A similar effect was described for BPA (Villar-Pazos et al., 2017), in which BPA exposure for 48 h decreased exocytosis at low glucose (5.6 mM) but increased exocytosis at high glucose concentrations (11 mM). While these findings suggest the existence of a crosstalk between BPA and glucose signaling effects on the exocytotic machinery, the existence of such crosstalk is yet to be elucidated. Exposure to BPF enhanced GSIS only at 1 µM, the same concentration at which gene expression occurred. These results emphasize the different potencies observed between BPS and BPF.

Our results in BERKO mice indicate that both BPS and BPF effects on gene expression are mediated by ERβ. BPF acts within the micromolar range, which is compatible with its ERβ affinity (see below). On the other hand, our data also suggest that 1 nM BPS acts through ERβ, which is surprising if we consider that BPS binds to ERβ and activates the classic nuclear-initiated pathway at higher concentrations. In vitro bioassays using the stably transfected HELN-hERβ cell line, which contains a luciferase gene driven by an ERE under the control of hERβ, have clearly demonstrated that BPA, BPS and BPF behaved as full hERβ agonists with potencies in the following order: BPA>BPF>BPS (Molina-Molina et al., 2013). Additionally, whole-cell competitive binding assays using the same cell line showed IC_{50} values of 0.21±0.01 nM (E2), 401±126 nM (BPA), 1452±261 nM (BPF), and 3452±878 nM (BPS) (Molina-Molina et al., 2013). Although our findings with BPF are compatible with this classic model, this does not seem to be the case for BPA and BPS.

We pointed out in the first part of the Discussion that low doses of bisphenols can signal through extranuclear-initiated pathways in β-cells. We showed that, like bisphenols, PaPE-1 is an agonist that uses this extranuclear pathway to decrease K_{ATP} channel activity in an ERβ-dependent manner. Then, it is possible that an extranuclear-initiated pathway may be implied in bisphenols action to explain their effects at nanomolar concentrations.

As already discussed, the efficacy of bisphenol response would depend on the interaction between ERβ and other proteins involved in extranuclear signaling. Molecular dynamics indicated that dimerization may be important and may explain, at least in part, why BPA and BPS are more potent than BPF. Dimerization is a requisite for ER extranuclear signaling (Razandi et al., 2004; Levin and Hammes, 2016) and its role deserves further research in the case of bisphenols and other xenoestrogens. Extranuclear signaling by nuclear receptors is a complex phenomenon and there

468 are very few data showing the activation of such extranuclear pathways by endocrine-disrupting
469 chemicals, including bisphenols (Marino et al., 2012; Vinas and Watson, 2013; Nadal et al., 2018).
470 ERs acting through this pathway do not directly engage DNA to regulate transcription but induce
471 non-nuclear signaling cascades that may lead to transcriptional regulation. Extranuclear ERs
472 interact with a plethora of signaling proteins associated to the plasma membrane or present in the
473 cytosol, such as G proteins and other receptors and kinases involved in extranuclear-initiated
474 signaling triggered by estrogens (Levin and Hammes, 2016). These interactions may amplify
475 bisphenol response via extranuclear ERβ as it has been shown for adrenergic and cholinergic
476 receptors, which respond to ultralow concentrations of ligand within the femtomolar range
477 (Civciristov et al., 2018). Thus, it is necessary to further study bisphenol-activated extranuclear-
478 initiated ER signaling pathways to better understand the efficacy of the response. This information
479 is urgently needed to develop improved testing methods for extranuclear-initiated effects as well
480 as to fully explain how low doses of estrogenic endocrine-disrupting chemicals affect several
481 biological processes.
482
483 CONCLUSIONS
484 Both short- and long-term exposure to BPS and BPF increases glucose-induced insulin release,
485 which is a risk factor for T2D. A rapid response may be due to the closure of K_{ATP} channels, while
486 a long-term response seems to be via regulation of ion channel gene expression. As K_{ATP} channel
487 activity, gene expression of ion channel and insulin release are endpoints relatively easy to be
488 measured, we propose they should be considered key events to assess the potential hazards of
489 bisphenols.

In line with previous work with ERβ agonists and BPA, our findings with BERKO mice and PaPE-1 suggest that bisphenols act as ERβ agonists and activate an extranuclear-initiated pathway. ERβ affinity for BPA and BPS cannot easily explain the biological effects described in the present work and in previous reports. Our data with acute exposure indicate that efficacy may be more important than affinity to explain effects at low doses. More experimental data on dimerization and interaction of ERβ with other signaling molecules in its vicinity are needed to fully understand effects at low doses of bisphenols, especially on gene transcription. In any case, our data support that these bisphenols are not a safe alternative to BPA.

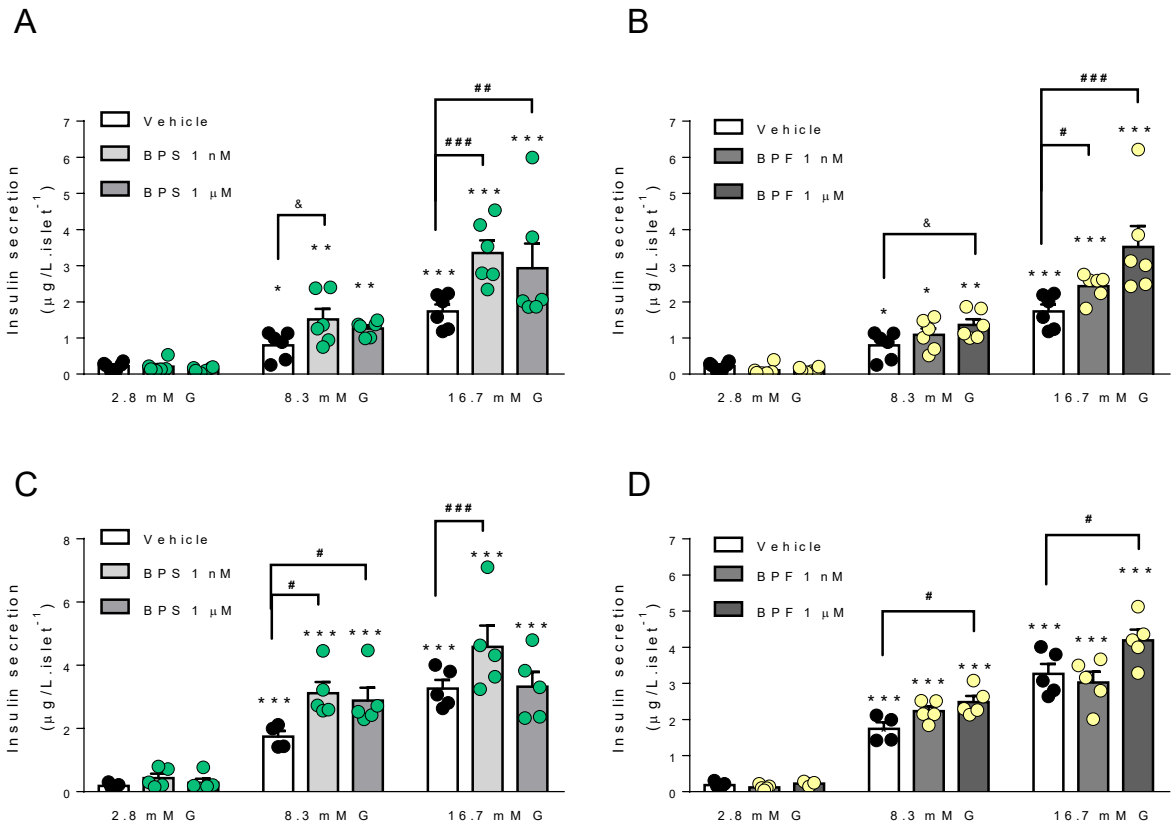

Figure 1. BPS and BPF increase glucose-stimulated insulin secretion in mouse islets. **(A-D)** Insulin secretion was measured at 2.8, 8.3 and 16.7 mM glucose in islets from C57BL/6J mice treated *ex vivo* with vehicle (control; black circles and white bars), 1 nM BPS (green circles and light grey bars) or BPF (yellow circles and light grey bars), or 1 µM BPS (green circles and dark grey bars) or BPF (yellow circles and dark grey bars). **(A and B)** After 2 h of recovery, treatments (vehicle, BPS or BPF) were added to each glucose solution so that the islets remained under treatment during the whole experiment. **(C and D)** Islets were treated *ex vivo* with vehicle BPS or BPF for 48 h, and then, glucose-stimulated insulin secretion was performed in the absence of treatments. Insulin release was measured by ELISA. Data are shown as means ± SEM of six independent islet preparations isolated on three different days: *p≤0.05, **p≤0.01, ***p≤0.001 vs 2.8 mM; $^{\#}$p≤0.05, $^{\#\#}$p≤0.01, $^{\#\#\#}$p≤0.001 comparisons indicated by bars (one-way ANOVA); $^{\&}$p≤0.05 (Student's t-test).

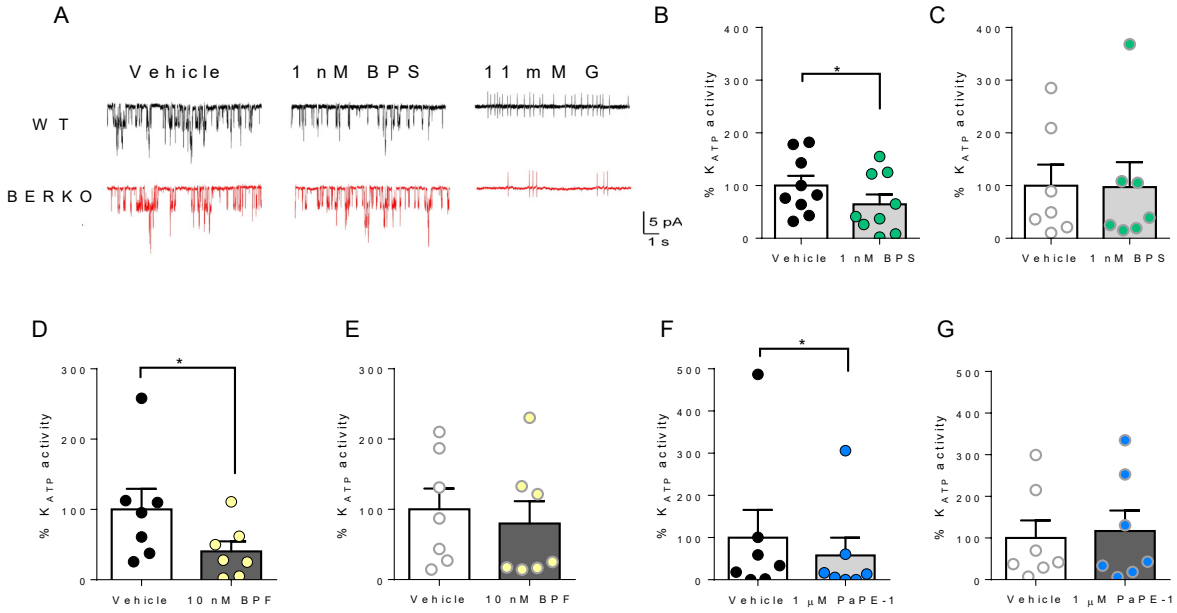

Figure 2. BPS, BPF and PaPE-1 block K_{ATP} channel activity in mouse pancreatic β-cells. (A) Representative recordings of K_{ATP} channel activity in β-cells isolated from wild-type (WT) (black traces) or BERKO (red traces) mice in control condition (0 mM glucose; vehicle; left column), in 1 nM BPS (middle column) and in 11 mM glucose (right). Channel openings are represented by downward deflections, reflecting inward currents due to the high K^+ content of the pipette. The abolition of K_{ATP} activity and generation of action currents at 11 mM glucose was used as a positive control of pancreatic β-cell identity (right column). **(B-G)** Quantification of the K_{ATP} channel activity in β-cells isolated from wild-type (WT) **(B, D and F)** or BERKO **(C, E and G)** mice treated *in vitro* with vehicle (black or white circles and white bars), 1 nM BPS (**B and C**; green circles and light grey bars), 10 nM BPF (**D and E**; yellow circles and dark grey bars) or 1 µM PaPE-1 (**F and G**; blue circles and black bars). The effect of three bisphenols was measured after 7±1 min of acute application. Data are represented as a percentage of activity with respect to resting conditions (0 mM Glucose). Experiments were carried out at 32-34ºC. Data are shown as means ± SEM of the number of cells recorded in WT (n=7-9 cells) and BERKO (n=7-9 cells) mice. These cells were isolated from three mice on three different days. *p≤0.05 vs control (Student's paired t-test).

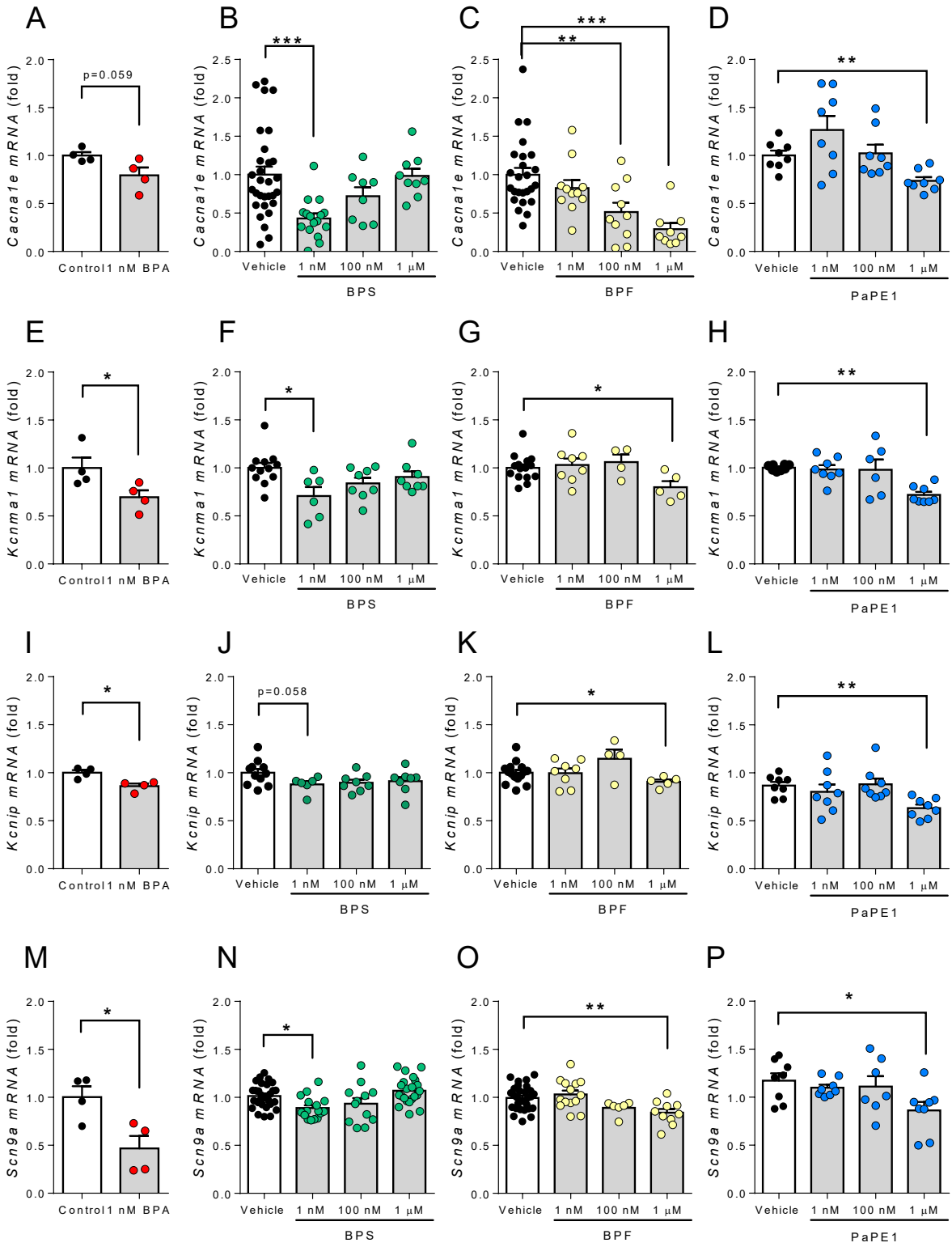

531

532 **Figure 3. BPA, BPS, BPF and PaPE-1 reduce *Cacna1e*, *Kcnma1*, *Kcnip* and *Scn9a* expression**
533 **in mouse islets**. mRNA expression of *Cacna1e* **(A-D)**, *Kcnma1* **()**, *Kcnip* **(I-L)** and *Scn9a* **(M-P)**

was measured in islets from C57BL/6J mice treated *ex vivo* with vehicle (control; black circles and white bars), BPA **(A, E, I and M**; red circles and light grey bars**),** BPS **(B, F, J and N**; green circles and light grey bars**)**, or BPF **(C, G, K and O**; yellow circles and light grey bars**)** or PaPE-1 **(D, H, L and P**; blue circles and light grey bars**)** at 1, 100 and 1000 nM for 48 h. mRNA expression was measured by qRT-PCR and normalized to the housekeeping gene *Hprt1,* and is shown as fold vs. mean of the controls. Data are shown as means ± SEM of four to twenty-nine independent samples from up to twenty-nine islets preparations isolated on at least three different days: *p≤0.05, **p≤0.01, ***p≤0.001 (ANOVA one way).

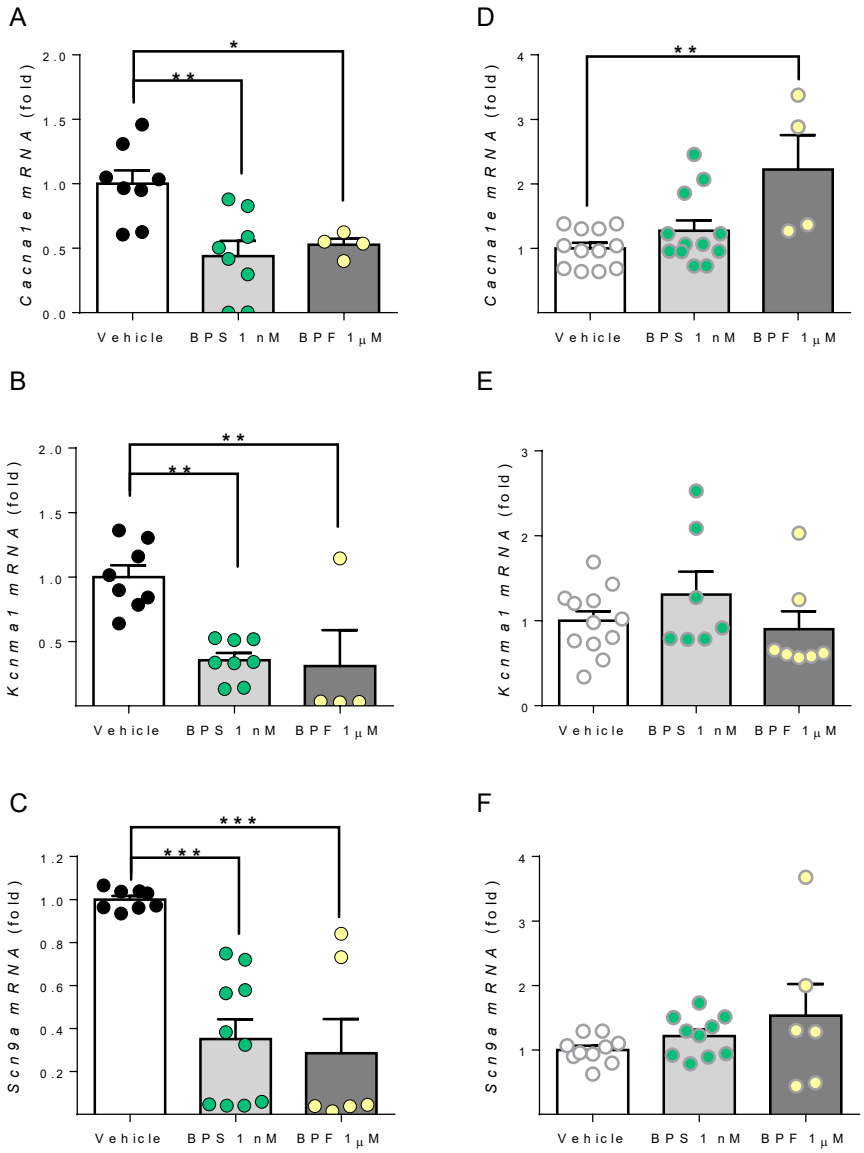

Figure 4. BPS, and BPF, reduce *Cacna1e*, *Kcnma1* and *Scn9a* expression in islets from wild type but not from BERKO mice. mRNA expression of *Cacna1e* **(A and D)**, *Kcnma1* **(B and E)** and *Scn9a* **(C and F)** in islets isolated from wild-type **(A, B and C)** or BERKO **(D, E and F)** mice treated *ex vivo* with vehicle (control; black circles and white bars), 1 nM BPS (green circles and light grey bars), or 1 µM BPF (yellow circles and dark grey bars) for 48 h. mRNA expression was measured by qRT-PCR and normalized to the housekeeping gene *Hprt1,* and is shown as fold vs mean of the controls. Data are shown as means ± SEM of four to eight independent islet preparations isolated on at least three different days: *p≤0.05, **p≤0.01, ***p≤0.001 (ANOVA one way).

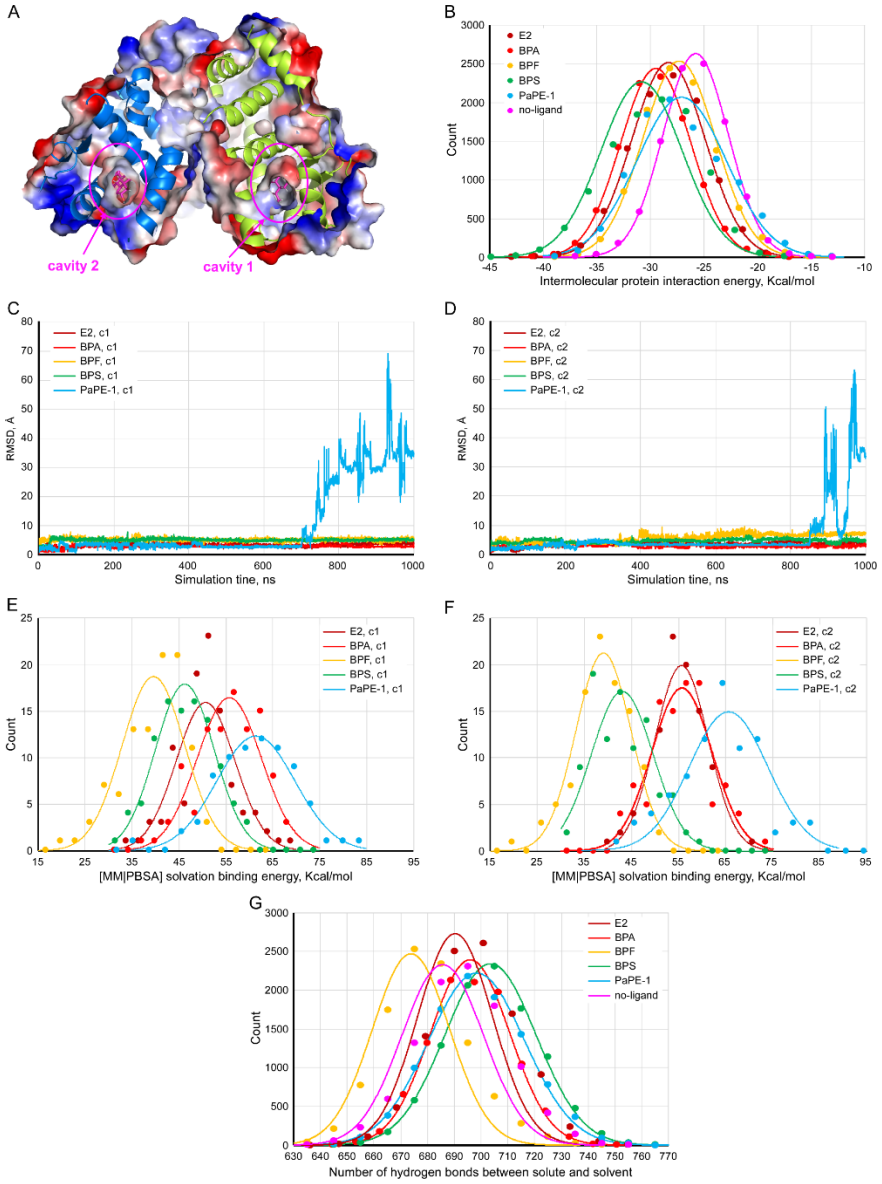

Figure 5. Molecular Dynamics. Analysis of trajectories, MM/PBSA solvation binding energies, and intermolecular interaction energies for the rERβ-ΔH12-LBD dimer from the data generated by MD simulations for 1 µs. **(A)** rERβ-ΔH12-LBD dimer secondary structure and electrostatic surface. The LBD cavity has been cut to show a bound ligand inside the structure. In the following panels, *c1* refers to cavity *1* and *c2* refers to *cavity 2*. **(B)** Frequency distributions of the intermolecular protein interaction energy for the subunits of the rERβ-ΔH12-LBD dimer in the presence of different ligands in each LBD cavity. **(C and D)** trajectories of the ligands (RMSD, Å) initially docked in cavity 1 **(C)** and 2 **(D)** of the LBD. **(E and F)** Frequency distributions of the MM/PBSA solvation binding energy values of each ligand attached to cavity 1 **(E)** and 2 **(F)**. **(G)** Frequency distribution of the number of H-bonds between the solute (protein) and the solvent. A Gaussian curve overlaps discrete data. The legends included within each panel indicate the different ligands analyzed.

AUTHOR INFORMATION

Corresponding Author

* Angel Nadal, Instituto de Investigación, Desarrollo e Innovación en Biotecnología Sanitaria de Elche (IDiBE), Universitas Miguel Hernández, 03202, Elche, Spain.

E-mail: nadal@umh.es

Author Contributions

LM: Conceptualization, Supervision, Investigation, Formal Analysis, Visualization, Writing - Review & Editing **JMP**: Conceptualization, Investigation, Formal Analysis, Visualization, Writing - Review & Editing **MCM**: Investigation, Formal Analysis, Visualization, Writing - Review & Editing **RSdS**: Investigation, Formal Analysis, Writing - Review & Editing **RMMG**: Investigation, Formal Analysis, Writing - Review & Editing **SS**: Investigation, Formal Analysis, Visualization, Writing - Review & Editing **IQ**: Visualization, Resources, Funding Acquisition, Writing - Review & Editing **J-AG**: Resources, Writing - Review & Editing **JAE**: Conceptualization, Investigation, Visualization, Resources, Funding Acquisition, Writing - Review & Editing **AN**: Conceptualization, Supervision, Visualization, Resources, Funding Acquisition, Writing - Original Draft, Project Administration. All authors have given approval to the final version of the manuscript.

Funding Sources

This work was supported by BPU2017-86579-R (AN) and BFU2016-77125-R (IQ) and RTI2018-096724-B-C21 (JAE) supported by FEDER/Ministerio de Ciencia e Innovación-Agencia Estatal de Investigación. PROMETEO/2020/006 (AN), PROMETEO/2016/006 (JAE) and SEJI/2018/023

589 (LM) supported by Generalitat Valenciana. J-AG was supported by the Robert A. Welch
590 Foundation (E-0004). CIBERDEM is an initiative of the Instituto de Salud Carlos III.

591

592 ACKNOWLEDGMENT

593 The authors thank Maria Luisa Navarro, Salomé Ramon, and Beatriz Bonmati Botella for their
594 excellent technical assistance. We are grateful to the Cluster of Scientific Computing
595 (http://ccc.umh.es/) of the Universitas Miguel Hernández for providing computing facilities.

596

597 REFERENCES

598 Acconcia, F., Pallottini, V., Marino, M., 2015. Molecular Mechanisms of Action of BPA. Dose
599 Response 13, 1559325815610582.
600 Alonso-Magdalena, P., Morimoto, S., Ripoll, C., Fuentes, E., Nadal, A., 2006. The estrogenic
601 effect of bisphenol A disrupts pancreatic beta-cell function in vivo and induces insulin resistance.
602 Environ Health Perspect 114, 106-112.
603 Alonso-Magdalena, P., Quesada, I., Nadal, A., 2011. Endocrine disruptors in the etiology of type
604 2 diabetes mellitus. Nat Rev Endocrinol 7, 346-353.
605 Alonso-Magdalena, P., Ropero, A.B., Carrera, M.P., Cederroth, C.R., Baquie, M., Gauthier, B.R.,
606 Nef, S., Stefani, E., Nadal, A., 2008. Pancreatic insulin content regulation by the estrogen receptor
607 ER alpha. PLoS One 3, e2069.
608 American Diabetes, A., 2018. 2. Classification and Diagnosis of Diabetes: Standards of Medical
609 Care in Diabetes-2018. Diabetes Care 41, S13-S27.
610 Ascenzi, P., Bocedi, A., Marino, M., 2006. Structure-function relationship of estrogen receptor
611 alpha and beta: impact on human health. Mol Aspects Med 27, 299-402.
612 Ashcroft, F.M., 2005. ATP-sensitive potassium channelopathies: focus on insulin secretion. J Clin
613 Invest 115, 2047-2058.
614 Batista, T.M., Alonso-Magdalena, P., Vieira, E., Amaral, M.E., Cederroth, C.R., Nef, S., Quesada,
615 I., Carneiro, E.M., Nadal, A., 2012. Short-term treatment with bisphenol-A leads to metabolic
616 abnormalities in adult male mice. PLoS One 7, e33814.
617 Beausoleil, C., Emond, C., Cravedi, J.P., Antignac, J.P., Applanat, M., Appenzeller, B.R.,
618 Beaudouin, R., Belzunces, L.P., Canivenc-Lavier, M.C., Chevalier, N., Chevrier, C., Elefant, E.,
619 Eustache, F., Habert, R., Kolf-Clauw, M., Le Magueresse-Battistoni, B., Mhaouty-Kodja, S.,
620 Minier, C., Multigner, L., Schroeder, H., Thonneau, P., Viguie, C., Pouzaud, F., Ormsby, J.N.,
621 Rousselle, C., Verines-Jouin, L., Pasquier, E., Michel, C., 2018. Regulatory identification of BPA
622 as an endocrine disruptor: Context and methodology. Mol Cell Endocrinol 475, 4-9.

623 Beydoun, H.A., Khanal, S., Zonderman, A.B., Beydoun, M.A., 2014. Sex differences in the
624 association of urinary bisphenol-A concentration with selected indices of glucose homeostasis
625 among U.S. adults. Ann Epidemiol 24, 90-97.
626 Biasini, M., Bienert, S., Waterhouse, A., Arnold, K., Studer, G., Schmidt, T., Kiefer, F., Gallo
627 Cassarino, T., Bertoni, M., Bordoli, L., Schwede, T., 2014. SWISS-MODEL: modelling protein
628 tertiary and quaternary structure using evolutionary information. Nucleic Acids Res 42, W252-
629 258.
630 Boronat-Belda, T., Ferrero, H., Al-Abdulla, R., Quesada, I., Gustafsson, J.A., Nadal, A., Alonso-
631 Magdalena, P., 2020. BISPHENOL-A EXPOSURE DURING PREGNANCY ALTERS
632 PANCREATIC beta-CELL DIVISION AND MASS IN MALE MICE OFFSPRING: A ROLE
633 FOR ERbeta. Food Chem Toxicol, 111681.
634 Celik, L., Lund, J.D., Schiott, B., 2007. Conformational dynamics of the estrogen receptor alpha:
635 molecular dynamics simulations of the influence of binding site structure on protein dynamics.
636 Biochemistry 46, 1743-1758.
637 Chen, L., Chen, J., Zhou, G., Wang, Y., Xu, C., Wang, X., 2016. Molecular Dynamics Simulations
638 of the Permeation of Bisphenol A and Pore Formation in a Lipid Membrane. Sci Rep 6, 33399.
639 Civciristov, S., Ellisdon, A.M., Suderman, R., Pon, C.K., Evans, B.A., Kleifeld, O., Charlton, S.J.,
640 Hlavacek, W.S., Canals, M., Halls, M.L., 2018. Preassembled GPCR signaling complexes mediate
641 distinct cellular responses to ultralow ligand concentrations. Sci Signal 11.
642 Colquhoun, D., 1998. Binding, gating, affinity and efficacy: the interpretation of structure-activity
643 relationships for agonists and of the effects of mutating receptors. Br J Pharmacol 125, 924-947.
644 Corkey, B.E., 2012. Banting lecture 2011: hyperinsulinemia: cause or consequence? Diabetes 61,
645 4-13.
646 Delfosse, V., Grimaldi, M., Pons, J.L., Boulahtouf, A., le Maire, A., Cavailles, V., Labesse, G.,
647 Bourguet, W., Balaguer, P., 2012. Structural and mechanistic insights into bisphenols action
648 provide guidelines for risk assessment and discovery of bisphenol A substitutes. Proc Natl Acad
649 Sci U S A 109, 14930-14935.
650 Delgado, J., Radusky, L.G., Cianferoni, D., Serrano, L., 2019. FoldX 5.0: working with RNA,
651 small molecules and a new graphical interface. Bioinformatics 35, 4168-4169.
652 Duan, Y., Yao, Y., Wang, B., Han, L., Wang, L., Sun, H., Chen, L., 2018. Association of urinary
653 concentrations of bisphenols with type 2 diabetes mellitus: A case-control study. Environ Pollut
654 243, 1719-1726.
655 Encinar, J.A., Fernandez-Ballester, G., Galiano-Ibarra, V., Micol, V., 2015. In silico approach for
656 the discovery of new PPARgamma modulators among plant-derived polyphenols. Drug Des Devel
657 Ther 9, 5877-5895.
658 Erion, K.A., Corkey, B.E., 2017. Hyperinsulinemia: a Cause of Obesity? Curr Obes Rep 6, 178-
659 186.
660 Ferguson, M., Lorenzen-Schmidt, I., Pyle, W.G., 2019. Bisphenol S rapidly depresses heart
661 function through estrogen receptor-beta and decreases phospholamban phosphorylation in a sex-
662 dependent manner. Sci Rep 9, 15948.
663 Fratev, F., 2015. Activation helix orientation of the estrogen receptor is mediated by receptor
664 dimerization: evidence from molecular dynamics simulations. Phys Chem Chem Phys 17, 13403-
665 13420.
666 Galiano, V., Garcia-Valtanen, P., Micol, V., Encinar, J.A., 2016. Looking for inhibitors of the
667 dengue virus NS5 RNA-dependent RNA-polymerase using a molecular docking approach. Drug
668 Des Devel Ther 10, 3163-3181.

669 Gao, X., Ma, J., Chen, Y., Wang, H.S., 2015. Rapid responses and mechanism of action for low-
670 dose bisphenol S on ex vivo rat hearts and isolated myocytes: evidence of female-specific
671 proarrhythmic effects. Environ Health Perspect 123, 571-578.
672 Gore, A.C., Chappell, V.A., Fenton, S.E., Flaws, J.A., Nadal, A., Prins, G.S., Toppari, J., Zoeller,
673 R.T., 2015. EDC-2: The Endocrine Society's Second Scientific Statement on Endocrine-Disrupting
674 Chemicals. Endocr Rev 36, E1-E150.
675 Hagobian, T.A., Bird, A., Stanelle, S., Williams, D., Schaffner, A., Phelan, S., 2019. Pilot Study
676 on the Effect of Orally Administered Bisphenol A on Glucose and Insulin Response in Nonobese
677 Adults. J Endocr Soc 3, 643-654.
678 Heldring, N., Pike, A., Andersson, S., Matthews, J., Cheng, G., Hartman, J., Tujague, M., Strom,
679 A., Treuter, E., Warner, M., Gustafsson, J.A., 2007. Estrogen receptors: how do they signal and
680 what are their targets. Physiol Rev 87, 905-931.
681 Hiriart, M., Velasco, M., Larque, C., Diaz-Garcia, C.M., 2014. Metabolic syndrome and ionic
682 channels in pancreatic beta cells. Vitam Horm 95, 87-114.
683 Holz, G.G.t., Kuhtreiber, W.M., Habener, J.F., 1993. Pancreatic beta-cells are rendered glucose-
684 competent by the insulinotropic hormone glucagon-like peptide-1(7-37). Nature 361, 362-365.
685 Jacobson, D.A., Shyng, S.L., 2020. Ion Channels of the Islets in Type 2 Diabetes. J Mol Biol 432,
686 1326-1346.
687 Jacobson, M.H., Woodward, M., Bao, W., Liu, B., Trasande, L., 2019. Urinary Bisphenols and
688 Obesity Prevalence Among U.S. Children and Adolescents. J Endocr Soc 3, 1715-1726.
689 Jereva, D., Fratev, F., Tsakovska, I., Alov, P., Pencheva, T., Pajeva, I., 2017. Molecular dynamics
690 simulation of the human estrogen receptor alpha: contribution to the pharmacophore of the
691 agonists. Mathematics and Computers in Simulation 133, 124-134.
692 Keminer, O., Teigeler, M., Kohler, M., Wenzel, A., Arning, J., Kassner, F., Windshugel, B.,
693 Eilebrecht, E., 2019. A tiered high-throughput screening approach for evaluation of estrogen and
694 androgen receptor modulation by environmentally relevant bisphenol A substitutes. Sci Total
695 Environ, 134743.
696 Kolla, S., Morcos, M., Martin, B., Vandenberg, L.N., 2018. Low dose bisphenol S or ethinyl
697 estradiol exposures during the perinatal period alter female mouse mammary gland development.
698 Reprod Toxicol 78, 50-59.
699 Krege, J.H., Hodgin, J.B., Couse, J.F., Enmark, E., Warner, M., Mahler, J.F., Sar, M., Korach,
700 K.S., Gustafsson, J.A., Smithies, O., 1998. Generation and reproductive phenotypes of mice
701 lacking estrogen receptor beta. Proc Natl Acad Sci U S A 95, 15677-15682.
702 Lang, I.A., Galloway, T.S., Scarlett, A., Henley, W.E., Depledge, M., Wallace, R.B., Melzer, D.,
703 2008. Association of urinary bisphenol A concentration with medical disorders and laboratory
704 abnormalities in adults. JAMA 300, 1303-1310.
705 Le Magueresse-Battistoni, B., Multigner, L., Beausoleil, C., Rousselle, C., 2018. Effects of
706 bisphenol A on metabolism and evidences of a mode of action mediated through endocrine
707 disruption. Mol Cell Endocrinol 475, 74-91.
708 Levin, E.R., Hammes, S.R., 2016. Nuclear receptors outside the nucleus: extranuclear signalling
709 by steroid receptors. Nat Rev Mol Cell Biol 17, 783-797.
710 Li, Y., Perera, L., Coons, L.A., Burns, K.A., Tyler Ramsey, J., Pelch, K.E., Houtman, R., van
711 Beuningen, R., Teng, C.T., Korach, K.S., 2018. Differential in Vitro Biological Action,
712 Coregulator Interactions, and Molecular Dynamic Analysis of Bisphenol A (BPA), BPAF, and
713 BPS Ligand-ERalpha Complexes. Environ Health Perspect 126, 017012.

714 Liao, C., Liu, F., Alomirah, H., Loi, V.D., Mohd, M.A., Moon, H.B., Nakata, H., Kannan, K.,
715 2012a. Bisphenol S in urine from the United States and seven Asian countries: occurrence and
716 human exposures. Environ Sci Technol 46, 6860-6866.
717 Liao, C., Liu, F., Guo, Y., Moon, H.B., Nakata, H., Wu, Q., Kannan, K., 2012b. Occurrence of
718 eight bisphenol analogues in indoor dust from the United States and several Asian countries:
719 implications for human exposure. Environ Sci Technol 46, 9138-9145.
720 Liu, B., Lehmler, H.J., Sun, Y., Xu, G., Sun, Q., Snetselaar, L.G., Wallace, R.B., Bao, W., 2019.
721 Association of Bisphenol A and Its Substitutes, Bisphenol F and Bisphenol S, with Obesity in
722 United States Children and Adolescents. Diabetes Metab J 43, 59-75.
723 Madak-Erdogan, Z., Kim, S.H., Gong, P., Zhao, Y.C., Zhang, H., Chambliss, K.L., Carlson, K.E.,
724 Mayne, C.G., Shaul, P.W., Korach, K.S., Katzenellenbogen, J.A., Katzenellenbogen, B.S., 2016.
725 Design of pathway preferential estrogens that provide beneficial metabolic and vascular effects
726 without stimulating reproductive tissues. Sci Signal 9, ra53.
727 Malaise, Y., Lencina, C., Cartier, C., Olier, M., Menard, S., Guzylack-Piriou, L., 2020. Perinatal
728 oral exposure to low doses of bisphenol A, S or F impairs immune functions at intestinal and
729 systemic levels in female offspring mice. Environ Health 19, 93.
730 Marino, M., Pellegrini, M., La Rosa, P., Acconcia, F., 2012. Susceptibility of estrogen receptor
731 rapid responses to xenoestrogens: Physiological outcomes. Steroids 77, 910-917.
732 Martinez-Pinna, J., Marroqui, L., Hmadcha, A., Lopez-Beas, J., Soriano, S., Villar-Pazos, S.,
733 Alonso-Magdalena, P., Dos Santos, R.S., Quesada, I., Martin, F., Soria, B., Gustafsson, J.A.,
734 Nadal, A., 2019. Oestrogen receptor beta mediates the actions of bisphenol-A on ion channel
735 expression in mouse pancreatic beta cells. Diabetologia 62, 1667-1680.
736 Molina-Molina, J.M., Amaya, E., Grimaldi, M., Saenz, J.M., Real, M., Fernandez, M.F., Balaguer,
737 P., Olea, N., 2013. In vitro study on the agonistic and antagonistic activities of bisphenol-S and
738 other bisphenol-A congeners and derivatives via nuclear receptors. Toxicol Appl Pharmacol 272,
739 127-136.
740 Mustieles, V., D'Cruz, S.C., Couderq, S., Rodriguez-Carrillo, A., Fini, J.B., Hofer, T., Steffensen,
741 I.L., Dirven, H., Barouki, R., Olea, N., Fernandez, M.F., David, A., 2020. Bisphenol A and its
742 analogues: A comprehensive review to identify and prioritize effect biomarkers for human
743 biomonitoring. Environ Int 144, 105811.
744 Nadal, A., Alonso-Magdalena, P., Soriano, S., Quesada, I., Ropero, A.B., 2009. The pancreatic
745 beta-cell as a target of estrogens and xenoestrogens: Implications for blood glucose homeostasis
746 and diabetes. Mol Cell Endocrinol 304, 63-68.
747 Nadal, A., Fuentes, E., Ripoll, C., Villar-Pazos, S., Castellano-Munoz, M., Soriano, S., Martinez-
748 Pinna, J., Quesada, I., Alonso-Magdalena, P., 2018. Extranuclear-initiated estrogenic actions of
749 endocrine disrupting chemicals: Is there toxicology beyond paracelsus? J Steroid Biochem Mol
750 Biol 176, 16-22.
751 Nadal, A., Soria, B., 1997. Glucose metabolism regulates cytosolic Ca2+ in the pancreatic beta-
752 cell by three different mechanisms. Adv Exp Med Biol 426, 235-243.
753 Pike, A.C.W., Brzozowski, A.M., Walton, J., Hubbard, R.E., Thorsell, A.-G., Li, Y.-L.,
754 Gustafsson, J.-Å., Carlquist, M., 2001. Structural Insights into the Mode of Action of a Pure
755 Antiestrogen. Structure 9, 145-153.
756 Quesada, I., Fuentes, E., Viso-Leon, M.C., Soria, B., Ripoll, C., Nadal, A., 2002. Low doses of the
757 endocrine disruptor bisphenol-A and the native hormone 17beta-estradiol rapidly activate
758 transcription factor CREB. FASEB J 16, 1671-1673.

759 Ranciere, F., Botton, J., Slama, R., Lacroix, M.Z., Debrauwer, L., Charles, M.A., Roussel, R.,
760 Balkau, B., Magliano, D.J., Group, D.E.S.I.R.S., 2019. Exposure to Bisphenol A and Bisphenol S
761 and Incident Type 2 Diabetes: A Case-Cohort Study in the French Cohort D.E.S.I.R. Environ
762 Health Perspect 127, 107013.
763 Razandi, M., Pedram, A., Merchenthaler, I., Greene, G.L., Levin, E.R., 2004. Plasma membrane
764 estrogen receptors exist and functions as dimers. Mol Endocrinol 18, 2854-2865.
765 Rochester, J.R., Bolden, A.L., 2015. Bisphenol S and F: A Systematic Review and Comparison of
766 the Hormonal Activity of Bisphenol A Substitutes. Environ Health Perspect 123, 643-650.
767 Ropero, A.B., Alonso-Magdalena, P., Garcia-Garcia, E., Ripoll, C., Fuentes, E., Nadal, A., 2008.
768 Bisphenol-A disruption of the endocrine pancreas and blood glucose homeostasis. Int J Androl 31,
769 194-200.
770 Ropero, A.B., Fuentes, E., Rovira, J.M., Ripoll, C., Soria, B., Nadal, A., 1999. Non-genomic
771 actions of 17beta-oestradiol in mouse pancreatic beta-cells are mediated by a cGMP-dependent
772 protein kinase. J Physiol 521 Pt 2, 397-407.
773 Rorsman, P., Ashcroft, F.M., 2018. Pancreatic beta-Cell Electrical Activity and Insulin Secretion:
774 Of Mice and Men. Physiol Rev 98, 117-214.
775 Ruiz-Torres, V., Losada-Echeberria, M., Herranz-Lopez, M., Barrajon-Catalan, E., Galiano, V.,
776 Micol, V., Encinar, J.A., 2018. New Mammalian Target of Rapamycin (mTOR) Modulators
777 Derived from Natural Product Databases and Marine Extracts by Using Molecular Docking
778 Techniques. Mar Drugs 16.
779 Salentin, S., Schreiber, S., Haupt, V.J., Adasme, M.F., Schroeder, M., 2015. PLIP: fully automated
780 protein-ligand interaction profiler. Nucleic Acids Res 43, W443-447.
781 Santin, I., Dos Santos, R.S., Eizirik, D.L., 2016. Pancreatic Beta Cell Survival and Signaling
782 Pathways: Effects of Type 1 Diabetes-Associated Genetic Variants. Methods Mol Biol 1433, 21-
783 54.
784 Shankar, A., Teppala, S., 2011. Relationship between urinary bisphenol A levels and diabetes
785 mellitus. J Clin Endocrinol Metab 96, 3822-3826.
786 Shtaiwi, A., Adnan, R., Khairuddean, M., Al-Qattan, M., 2018. Molecular dynamics simulation of
787 human estrogen receptor free and bound to morpholine ether benzophenone inhibitor. Theor.
788 Chem. Acc. 137, 10.
789 Smith, C.L., O'Malley, B.W., 2004. Coregulator function: a key to understanding tissue specificity
790 of selective receptor modulators. Endocr Rev 25, 45-71.
791 Soriano, S., Alonso-Magdalena, P., Garcia-Arevalo, M., Novials, A., Muhammed, S.J., Salehi, A.,
792 Gustafsson, J.A., Quesada, I., Nadal, A., 2012. Rapid insulinotropic action of low doses of
793 bisphenol-A on mouse and human islets of Langerhans: role of estrogen receptor beta. PLoS One
794 7, e31109.
795 Soriano, S., Ropero, A.B., Alonso-Magdalena, P., Ripoll, C., Quesada, I., Gassner, B., Kuhn, M.,
796 Gustafsson, J.A., Nadal, A., 2009. Rapid regulation of K(ATP) channel activity by 17{beta}-
797 estradiol in pancreatic {beta}-cells involves the estrogen receptor {beta} and the atrial natriuretic
798 peptide receptor. Mol Endocrinol 23, 1973-1982.
799 Soto, A.M., Schaeberle, C., Maier, M.S., Sonnenschein, C., Maffini, M.V., 2017. Evidence of
800 Absence: Estrogenicity Assessment of a New Food-Contact Coating and the Bisphenol Used in Its
801 Synthesis. Environ Sci Technol 51, 1718-1726.
802 Stahlhut, R.W., Myers, J.P., Taylor, J.A., Nadal, A., Dyer, J.A., Vom Saal, F.S., 2018.
803 Experimental BPA Exposure and Glucose-Stimulated Insulin Response in Adult Men and Women.
804 J Endocr Soc 2, 1173-1187.

805 Valdeolmillos, M., Nadal, A., Contreras, D., Soria, B., 1992. The relationship between glucose-
806 induced K+ATP channel closure and the rise in [Ca2+]i in single mouse pancreatic beta-cells. J
807 Physiol 455, 173-186.
808 Vettorazzi, J.F., Ribeiro, R.A., Borck, P.C., Branco, R.C., Soriano, S., Merino, B., Boschero, A.C.,
809 Nadal, A., Quesada, I., Carneiro, E.M., 2016. The bile acid TUDCA increases glucose-induced
810 insulin secretion via the cAMP/PKA pathway in pancreatic beta cells. Metabolism 65, 54-63.
811 Villar-Pazos, S., Martinez-Pinna, J., Castellano-Munoz, M., Alonso-Magdalena, P., Marroqui, L.,
812 Quesada, I., Gustafsson, J.A., Nadal, A., 2017. Molecular mechanisms involved in the non-
813 monotonic effect of bisphenol-a on ca2+ entry in mouse pancreatic beta-cells. Sci Rep 7, 11770.
814 Vinas, R., Watson, C.S., 2013. Bisphenol S disrupts estradiol-induced nongenomic signaling in a
815 rat pituitary cell line: effects on cell functions. Environ Health Perspect 121, 352-358.
816 Wetherill, Y.B., Akingbemi, B.T., Kanno, J., McLachlan, J.A., Nadal, A., Sonnenschein, C.,
817 Watson, C.S., Zoeller, R.T., Belcher, S.M., 2007. In vitro molecular mechanisms of bisphenol A
818 action. Reprod Toxicol 24, 178-198.
819 Ye, X., Wong, L.Y., Kramer, J., Zhou, X., Jia, T., Calafat, A.M., 2015. Urinary Concentrations of
820 Bisphenol A and Three Other Bisphenols in Convenience Samples of U.S. Adults during 2000-
821 2014. Environ Sci Technol 49, 11834-11839.
822 Zhang, Z., Hu, Y., Guo, J., Yu, T., Sun, L., Xiao, X., Zhu, D., Nakanishi, T., Hiromori, Y., Li, J.,
823 Fan, X., Wan, Y., Cheng, S., Li, J., Guo, X., Hu, J., 2017. Fluorene-9-bisphenol is anti-oestrogenic
824 and may cause adverse pregnancy outcomes in mice. Nat Commun 8, 14585.

825